

## Resonance Neutron Capture and Transmission in Sulfur, Iron, and Lead\*

R. L. MACKLIN, P. J. PASMA,† AND J. H. GIBBONS

Oak Ridge National Laboratory, Oak Ridge, Tennessee

(Received 29 June 1964)

Resonances in both the capture and total cross sections for  $^{32}\text{S}$ ,  $^{56}\text{Fe}$ ,  $^{206}\text{Pb}$ ,  $^{207}\text{Pb}$ , and  $^{208}\text{Pb}$  were investigated in the energy range from 10 to 80 keV. Total and radiative widths, and in some cases spins and/or parities, were assigned, and isotopic identifications of resonances were made. Previously unknown resonances mostly due to  $l>0$  neutrons, were found in all of these nuclei. The  $p$ -wave level density for  $^{206}\text{Pb}$  and  $^{207}\text{Pb}$  was found to be more than twice as high as one would expect from the number of observed  $s$  resonances. The total radiative widths for an  $l_n=0$  versus two  $l_n=1$  resonances for  $^{207}\text{Pb}$  targets differed by a factor of 10. The effective nuclear radius,  $R'$ , was found to be  $(8.5\pm 0.2)F$  ( $^{206}\text{Pb}$ ),  $(9.5\pm 0.3)F$  ( $^{207}\text{Pb}$ ), and  $(8.4\pm 0.3)F$  ( $^{208}\text{Pb}$ ), giving an average of  $(8.8\pm 0.3)F$  which is in good agreement with an optical-model prediction of  $8.7F$ .

### I. INTRODUCTION

NEUTRON interactions with nuclei are simplest at very low energies where only  $l=0$  interactions can occur, resulting in pure  $s$ -wave elastic scattering and capture. In the keV range, while one is generally still below threshold for inelastic scattering, scattering and capture from  $l=1$  partial waves frequently are important. In fact, while the centrifugal barrier keeps the  $l=1$  scattering width small in comparison with  $l=0$ , the capture cross section can be dominated by  $l=1$  resonances which are virtually unobservable in the total cross section.

Studies of radiative capture using a large liquid scintillator<sup>1</sup> indicated the possible presence of a resonance near 30 keV in sulfur, and near 35 and 50 keV in iron.<sup>2</sup> We decided to investigate these nuclei in the energy regions mentioned since no resonance structure had been previously observed.

The resonance structure of the lead isotopes is of considerable interest, particularly in the calculation of the chronology of our galaxy.<sup>3-6</sup> Earlier investigations at Duke<sup>7,8</sup> and Oak Ridge National Laboratory (ORNL)<sup>9</sup> disclosed an appreciable number of resonances below 100 keV in lead, but that most were very weak. We chose to investigate these nuclides in an attempt to understand all resonance structure responsible for capture in this energy range.

### II. EXPERIMENTAL METHOD

The technique of pulsed-beam time-of-flight was used.<sup>10</sup> Proton pulses were supplied by the ORNL terminal-pulsed (and klystron-bunched) Van de Graaff.<sup>11</sup> In the case of total cross sections the proton pulse length,  $\leq 5$  nsec, was chosen to be compatible with the  $\text{B}_4^{10}\text{C}$ -NaI detector resolution ( $\sim 7$  nsec). The pulse rate was 500 kc/sec and the peak proton current was a few milliamperes. Neutrons were produced by the  $^7\text{Li}(p,n)^7\text{Be}$  reaction. Flight paths used varied from 1 to 3 m, resulting in a time resolution for neutrons of 3–10 nsec/m.

The time resolution of the detector<sup>12</sup> used to measure capture cross sections was about 2 nsec, and therefore proton pulses were bunched to  $\sim 1$  nsec with a repetition rate of 3 Mc/sec for this experiment. This advantage (short time resolution and high-repetition rate) was offset by the low-detection efficiency, which necessitated short flight paths. At the flight path used in these measurements (8 cm) the kinematic collimation of  $\text{Li}(p,n)$  neutrons near threshold was sufficient and no further collimation was used. The over-all time resolution for capture measurements was considerably poorer than that used in total cross-section measurements.

#### A. Samples

Physical properties of the samples are summarized in Table I. The enriched isotopes were supplied by the ORNL Isotopes Division. All samples were used in their elemental form. The capture cross section of tantalum was used as a standard in the capture measurements; flux was monitored by means of proton-current integration. Capture samples were circular disks or spherical shell segments matched with tantalum monitor disks. Transmission samples were right cylindrical sections.

<sup>10</sup> J. H. Neiler and W. M. Good, *Fast Neutron Physics* (Interscience Publishers, Inc., New York, 1960), Part I, p. 509.

<sup>11</sup> C. D. Moak, W. M. Good, R. F. King, J. W. Johnson, H. E. Banta, J. Judish, and W. H. DuPreez, *Rev. Sci. Instr.* **35**, 672 (1964).

<sup>12</sup> R. L. Macklin, J. H. Gibbons, and T. Inada, *Nucl. Phys.* **43**, 353 (1963).

\* Research sponsored by the U. S. Atomic Energy Commission under contract with the Union Carbide Corporation.

† Visiting scientist from Natuurkundig Laboratorium, Rijks-Universiteit, Groningen, The Netherlands.

<sup>1</sup> J. H. Gibbons, R. L. Macklin, P. D. Miller, and J. H. Neiler, *Phys. Rev.* **122**, 182 (1961).

<sup>2</sup> J. H. Gibbons, R. L. Macklin, P. D. Miller, and H. W. Schmitt, (unpublished results by private communication).

<sup>3</sup> E. M. Burbidge, G. R. Burbidge, W. A. Fowler, and F. Hoyle, *Rev. Mod. Phys.* **29**, 547 (1957).

<sup>4</sup> D. D. Clayton, W. A. Fowler, T. E. Hull, and B. A. Zimmerman, *Ann. Phys. (N.Y.)* **12**, 331 (1961).

<sup>5</sup> W. A. Fowler and F. Hoyle, *Ann. Phys. (N.Y.)* **10**, 280 (1960).

<sup>6</sup> D. D. Clayton, *Astrophys. J.* **139**, 637 (1964).

<sup>7</sup> H. W. Newson, J. H. Gibbons, H. Marshak, E. G. Bilpuch, R. H. Rohrer, and P. Capp, *Ann. Phys. (N.Y.)* **14**, 346 (1961).

<sup>8</sup> E. G. Bilpuch, K. K. Seth, C. D. Bowman, R. H. Tabony, R. C. Smith, and H. W. Newson, *Ann. Phys. (N.Y.)* **14**, 387 (1961).

<sup>9</sup> J. R. Bird, J. H. Gibbons, and W. M. Good, *Bull. Am. Phys. Soc.* **7**, 552 (1962).

TABLE I. Sample thicknesses and isotopic composition. Isotopic composition of samples is given below each constituent in atom percent. Samples used in capture versus total cross-section measurements are identified with a C or T in the last column.

Principal isotope (X)	Minor Isotopes				$N_x$ (atoms/b)	
S-32	S-33	S-34	S-36			
95.0	0.76	4.22	0.014	0.0105	C	
95.0	0.76	4.22	0.014	0.225	T	
Fe-56	Fe-54	Fe-57	Fe-58			
98.80	0.28	0.67	0.26	0.0535	T	
91.66	5.82	2.19	0.33	0.00654	C	
Fe-57	Fe-54	Fe-56	Fe-58			
91.19	0.14	8.53	0.14	0.00172	C	
Pb-206	Pb-204	Pb-207	Pb-208			
88.38	0.085	8.57	2.97	0.01568	C	
88.38	0.085	8.57	2.97	0.0683	T	
88.38	0.085	8.57	2.97	0.0341	T	
Pb-207	Pb-204	Pb-206	Pb-208			
87.71	0.1	4.74	7.44	0.01181	C	
92.85	<0.05	2.47	4.68	0.0612	T	
92.85	<0.05	2.47	4.68	0.0221	T	
Pb-208	Pb-204	Pb-206	Pb-207			
99.75	<0.05	0.20	<0.05	0.01821	C	

### B. Total Cross Sections

Data were taken at various flight paths, depending upon the energy range studied. During earlier experiments,<sup>13</sup> difficulties were encountered for  $E_n \geq 20$  keV due to neutrons that penetrated the boron slab and were captured in the iodine of the NaI crystal. Iodine-capture gamma-ray pulses that fell within the  $^{10}\text{B}(n,\gamma)$  "window" at 478 keV were counted, resulting in a spoiling of time resolution. This effect was largely eliminated by taking a background count, simultaneously with the foreground count, using a second "window" covering 0.5–5-MeV pulses from background as well as  $\text{I}(n,\gamma)$  pulses. Transmission data were not corrected for in-scattering since in by far the worst case ( $^{207}\text{Pb}$  at 42 keV) the observed peak cross section was reduced by about 5%.

All resonances were measured at least twice, more frequently three or four times at different flight paths. The results given in the figures are representative of the data obtained. The tabular results on resonance parameters (Table II) represent averages over the various runs, and we have attempted to include in the errors a reflection of the reproducibility of results.

### C. Capture Cross Sections

Samples used in the capture measurements were significantly thinner than those used in total cross section measurements. This was so for two principle reasons: (1) Scattering and self-shielding effects are very important corrections in capture measurements;

(2) the sample thickness needed to be kept a small fraction of the neutron flight path for optimum time resolution.

The capture cross sections were normalized to  $\sigma_c(\text{Ta})$  using the recipe  $\sigma(\text{Ta}) = 8600 \exp(-0.697 \ln E)$ , which is nearly identical with the solid curve in Ref. 1. The data were corrected for both average path length<sup>14</sup> (neutron scattering) and resonance self-shielding.<sup>15</sup> Observed widths of resonances were without exception much greater than the natural width. Resonance parameters were computed from the area under the capture curve. The observed cross sections were corrected for isotopic impurities by measuring all pertinent isotopes and iterating the results. Thus the capture results shown are for a pure isotope.

## III. RESULTS

### Sulfur

Previous measurements of the total cross section of sulfur disclosed no detectable resonance below the large  $s$ -wave resonance near 110 keV. However, our capture cross-section studies<sup>1</sup> near 30 and 65 keV gave a strong indication of a resonance in the vicinity of 30 keV, since the capture cross section near 30 keV was considerably larger than the 65-keV cross section. A relatively thick sample measurement<sup>12</sup> then confirmed the presence of a resonance in the region 25–30 keV, but it was impossible, because of the sample thickness, to determine its parameters accurately. The results for a thin-sample study of sulfur are given in Fig. 1.

A transmission measurement of this same resonance is given in Fig. 2. The resonance width is essentially the instrumental resolution. The peak is seen as a symmetric one (thus  $l_n \geq 1$ ) lying on a base of  $s$ -wave potential scattering that is falling with increasing energy because of interference with the  $s$  level at 110 keV. The two measurements combine to give the description of

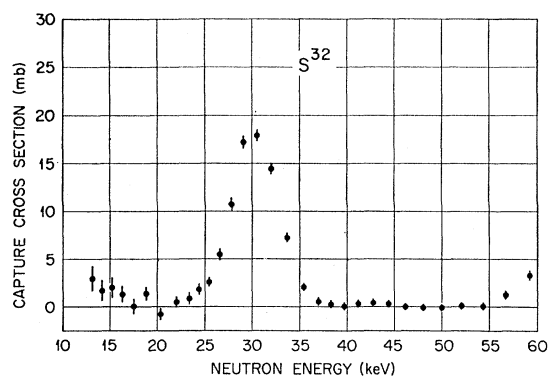


FIG. 1. Capture cross section of sulfur. The observed width of the resonance is due to experimental conditions (time-of-flight resolution and sample thickness).

<sup>14</sup> H. W. Schmitt, Oak Ridge National Laboratory Report ORNL 2883, 1960 (unpublished, but summarized in Ref. 1).

<sup>15</sup> R. L. Macklin, Nucl. Instr. Methods 26, 213 (1964).

<sup>13</sup> W. M. Good, J. H. Neiler, and J. H. Gibbons, Phys. Rev. 109, 926 (1958).

TABLE II. Summary of resonance parameters. Numbers given in parentheses represent weak resonances whose assignment is still somewhat uncertain. The differences between column 3 and 4 indicate the over-all effects of scattering, self-shielding, etc. When a choice of a given  $J$  is not certain, results for  $\Gamma$  and  $\Gamma_\gamma$  are given in terms of multiple choice and ( $g\Gamma_\gamma$ ). Angular momentum assignments were made on the basis of such observables as resonance symmetry and total width.

Target nucleus	$E_0$ (keV)	Observed $A(n,\gamma)$ (b eV)	Corrected $A(n,\gamma)$ (b eV)	$J^\pi$	$\Gamma$ (eV)	$g\Gamma_\gamma\Gamma_n/\Gamma$ (eV)	Remarks
$^{32}\text{S}$	$30.0\pm 0.3$	$117\pm 12$	$141\pm 15$	(?) <sup>-</sup>	$50\pm 10(J=\frac{1}{2}), 36\pm 8(J=\frac{3}{2})$	$g\Gamma_\gamma=1.0\pm 0.2$	$l=1$
$^{56}\text{Fe}$	22	$40\pm 30$	$43\pm 32$		Not observed ( $\Gamma < 10$ eV)	$0.2\pm 0.2$	
	28	$213\pm 30$	$226\pm 32$	$\frac{1}{2}^+$	(1600±100)	$\Gamma_\gamma=1.5\pm 0.3$	$l=0$
	36	$214\pm 22$	$227\pm 23$		Not observed ( $\Gamma < 10$ eV)	$1.9\pm 0.3$	
	50	$145\pm 45$	$155\pm 50$		$44\pm 8(J=\frac{1}{2}), 29\pm 6(J=\frac{3}{2})$	$g\Gamma_\gamma=1.9\pm 0.6$	$l=1$ or 2
$^{57}\text{Fe}$	12.7	$625\pm 65$	$665\pm 70$		Not observed	$2.0\pm 0.3$	
	17.0	$380\pm 80$	$380\pm 80$		Not observed	$1.5\pm 0.5$	
	20.5	$370\pm 80$	$370\pm 80$		Not observed	$1.8\pm 0.5$	
	27	$725\pm 73$	$745\pm 75$	$1^+$		$\Gamma_\gamma=6\pm 2$	$l=0$
$^{206}\text{Pb}$	(12.2)				$J=\frac{1}{2} \quad J=\frac{3}{2}$ $< 14 \quad < 10$ $< 20 \quad < 12$		( $l=1$ ) $l=1$
	$16.5\pm 0.3$	$140\pm 15$	$202\pm 22$	(?) <sup>-</sup>	Not observed	$g\Gamma_\gamma=0.80\pm 0.12$	$l=1$
	21	$27\pm 9$	$36\pm 12$			$0.18\pm 0.07$	
	$25.1\pm 0.4$	$96\pm 10$	$124\pm 13$	(?) <sup>-</sup>	$49\pm 10 \quad 34\pm 7$	$g\Gamma_\gamma=0.77\pm 0.12$	$l=1$
	35.0)			{(?) <sup>-</sup>	$58\pm 8 \quad 39\pm 6$	$g\Gamma_\gamma=0.85\pm 0.2$	{ $l=1$ $l=1$
	46.0)	$145\pm 15$	$158\pm 17$	{(?) <sup>-</sup>	$73\pm 9 \quad 48\pm 7$		
	$66\pm 2$			$\frac{1}{2}^+$	$250\pm 150$		$l=0$
	$75\pm 2$			(?) <sup>-</sup>	$50\pm 15 \quad 33\pm 10$		$l\geq 1$
$^{207}\text{Pb}$	(12.1)				$J=0 \quad J=1 \quad J=2$ $(25\pm 15) \quad (14\pm 8) \quad (11\pm 5)$		( $l=1$ )
	$16.7\pm 0.3$	$53\pm 6$	$74\pm 8$	(?) <sup>+</sup>	$91\pm 20 \quad 51\pm 10 \quad 36\pm 7$	$g\Gamma_\gamma=0.3\pm 0.07$	$l=1$
	$29\pm 0.4$	$44\pm 15$	$50\pm 17$	(?) <sup>+</sup>	$65\pm 15 \quad 30\pm 7 \quad 23\pm 6$	$g\Gamma_\gamma=0.35\pm 0.13$	$l=1$
	$37.0\pm 0.5$			(?) <sup>+</sup>	$70\pm 20 \quad 30\pm 8 \quad 22\pm 5$		$l=1$
	$41.2\pm 0.5$	$396\pm 40$	$413\pm 43$	$1^-$	$1100\pm 150$	$\Gamma_\gamma=5.5\pm 0.9$	$l=0$

the resonance found in Table II. The observed peak cross section and width eliminate any chance that the resonance is due to  $^{34}\text{S}$ . This conclusion is supported by recent capture  $\gamma$ -ray studies<sup>16</sup> which confirm the resonance to be in ( $^{32}\text{S}+n$ ).

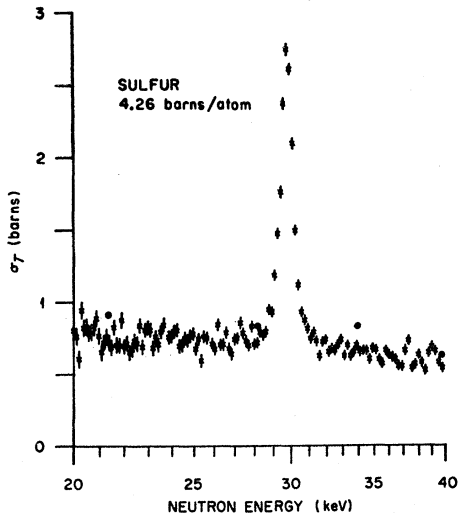


FIG. 2. Total cross section of sulfur near the 30-keV resonance. The observed width is due to instrumental resolution. This resonance is due to  $l=1$  neutrons on  $^{32}\text{S}$ . Solid circles are due to Adair, Bockelman, and Peterson, Phys. Rev. 76, 308 (1949).

<sup>16</sup> I. Bergqvist, W. M. Good, and J. H. Gibbons (private communication, 1963).

Iron-56

Total cross-section studies of iron have disclosed resonances in ( $^{56}\text{Fe}+n$ ) near 28.0, 74, and 84 keV.<sup>8,17</sup> A small resonance near 1.2 keV has also been reported.<sup>18-21</sup> The 1.2 keV resonance is extremely narrow ( $\Gamma_\gamma \approx \Gamma$ ) and has been assigned as  $J^\pi = \frac{1}{2}^+$ . The other three resonances are large and are clearly  $s$  wave. Our results for the capture cross section of  $^{56}\text{Fe}$  in the energy range  $14 < E_n < 60$  keV are given in Fig. 3. It is immediately clear that a major portion of capture in this energy range is due to resonances not previously observed in total cross sections. The results indicate resonances at  $\sim 22, \sim 27.5, 36,$  and  $51$  keV. The turn-up in cross section at both extremes of the curve indicate at least one additional resonance for  $10 < E_n < 15$  and  $E_n > 60$  keV. Transmission resonances have been observed in ( $^{54}\text{Fe}+n$ ) at 36 (weak), 53, and 72 keV.<sup>17</sup> The resonances we observed at 36 and 50 keV cannot be solely due to  $^{54}\text{Fe}$  since a reasonable assumption for radiative widths leads to a capture-area contribution from  $^{54}\text{Fe}$  of

<sup>17</sup> H. W. Newson, E. G. Bilpuch, F. P. Karriker, L. W. Weston, J. R. Patterson, and C. D. Bowman, Ann. Phys. 14, 365 (1961).

<sup>18</sup> A. I. Isakov, Yu. P. Popov, and F. L. Shapiro, Zh. Eksperim. i Teor. Fiz. 38, 989 (1960) [English transl.: Soviet Phys.—JETP 11, 712 (1960)].

<sup>19</sup> R. C. Block, J. E. Russell, and R. W. Hockenbury, Atomic Energy Research Establishment Report No. AERE-R-4131, 1962 (unpublished).

<sup>20</sup> M. C. Moxon and E. R. Rae, Atomic Energy Research Establishment Report No. AERE-R-4131, 1962 (unpublished).

<sup>21</sup> J. A. Moore, H. Palevsky, and R. E. Chrien, Phys. Rev. 132, 801 (1963).

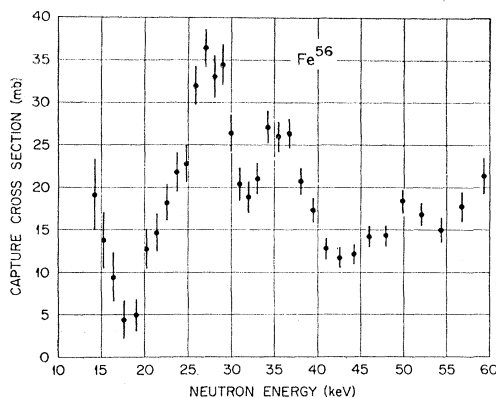


FIG. 3. Neutron capture cross section of  $^{56}\text{Fe}$ . The peak at 27.5 keV is due to a known  $J^\pi = \frac{1}{2}^+$ ,  $l_n = 0$  resonance. The other peaks are due to previously unobserved resonances, possibly due to  $l = 2$  neutrons.

only a few percent of that observed. A summary of resonance capture areas and possible radiative widths is given in Table II. The only resonance in this region for which a  $J^\pi$  has been assigned is the one at 28 keV. Our result for the radiative width,  $\Gamma_\gamma = 1.5 \pm 0.3$  eV, lies higher by about a factor of 2 than the corresponding width (0.67 eV) (Ref. 21) of the 1.2-keV resonance and higher by an even greater factor than average widths of resonances for slightly heavier nuclei.<sup>22</sup> The high ratio of scattering to capture at this resonance (nearly  $10^3$ ) does not appreciably interfere with the radiative width measurement for two reasons. First, the scattered neutrons travel nearly twice as far (to reach the detector) as the ones captured in the sample, and thus any counts they induced promptly in the detector would be about 10 resolution widths removed from the capture gamma-ray peak in the time spectrum. Secondly, an upper limit for the prompt detection efficiency of  $10^{-4}$  times the capture detection efficiency can be set from the statistical fluctuations of the background using a carbon scatterer. Because of the 3-Mc/sec repetition rate, scattered neutrons that have been appreciably slowed down or thermalized are spread over many cycles and included in the measured random time backgrounds. Widths of the resonances near 22 and 36 keV are given in terms of capture areas only since neither  $\Gamma$  nor  $J^\pi$  is known. The capture area under an isolated resonance is, of course, equal to  $(2\pi^2/k^2)g(\Gamma_n\Gamma_\gamma/\Gamma)$ . Capture area correction factors,<sup>23</sup> somewhat dependent upon  $J^\pi$  and  $\Gamma$ , were computed for a reasonable range of values and the consequent uncertainties included in the results.

A transmission measurement was performed using a thick sample of pure  $^{56}\text{Fe}$  in an attempt to measure the

total widths of these resonances. The observed transmission is shown in Fig. 4. The prominent feature is the well-known  $s$ -wave resonance near 28 keV. The results imply incorrectly  $E_0 \approx 27$  keV, owing to a timing fault; the true transmission minimum occurs more nearly at 28.0 keV. No indication of a resonance is seen near 22 and 36 keV, so that only upper limits may be stated for the width of these two resonances. However, a resonance does appear near 51 keV. Its symmetry implies  $l_n \geq 1$  and its width is consistent with either  $l = 1$  or  $l = 2$ . It is quite possible that some of these very narrow resonances are due to  $d$ -wave neutrons, since  $^{56}\text{Fe}$  lies near the  $3S$  (and therefore also probably the  $2D$ ) giant resonance maximum. The probability that these small resonances are  $p$  wave is lessened in that the  $p$ -wave strength function is small in this region.

The  $\gamma$ -ray spectra due to capture at 1200 eV, similar to thermal spectra, have been used to conclude<sup>21</sup> that the state is  $J^\pi = \frac{1}{2}^+$ ,  $l_n = 0$ . However, the observed spectra are quite consistent with and perhaps in even better agreement with an assignment  $J = \frac{3}{2}$ ; the 6.932-MeV transition reported by Moore *et al.*<sup>21</sup> significantly feeds the level at 0.707 MeV which has been recently reported<sup>24</sup> to have a spin  $J^\pi = \frac{5}{2}^-$ . If the 1200-eV resonance were  $p$  wave, all of the observed transitions would be type M1. If the resonance were due to  $d$ -wave neutrons an expected neutron width would be  $\lesssim 10$  MeV, which is not inconsistent with the reported width (25 meV for  $J = \frac{3}{2}$ ). In any case, we feel the reported abundance of the 6.932-MeV line casts serious doubt on the assignment  $l = 0$ .

### Iron-57

Total cross-section studies<sup>25</sup> of  $^{57}\text{Fe}$  have revealed,  $s$ -wave resonances at 3.7, 5.9, 12.7 (weak), 28.5, 40, and 48.5 keV. A preliminary transmission measurement in the range  $10 < E_n < 25$  keV revealed no evidence of additional resonances with  $\Gamma > 25$  eV. However, the capture cross section (Fig. 5) shows that there are at least three strongly capturing resonances for  $10 \leq E_n \leq 20$  keV and also evidence of resonance capture above 35 keV, in addition to capture corresponding to the known resonance at 28.5 keV. It is tempting to suggest that the strongly capturing resonances between 10 and 20 keV are due to  $d$ -wave neutrons, since the  $d$ -wave strength function should be large for  $A \approx 57$ , and a typical  $d$ -wave resonance near, for example, 20 keV should have a width of the order of 10 eV.

### Lead

The capture cross sections of the isotopes of lead are very important in cosmic chronology (sometimes re-

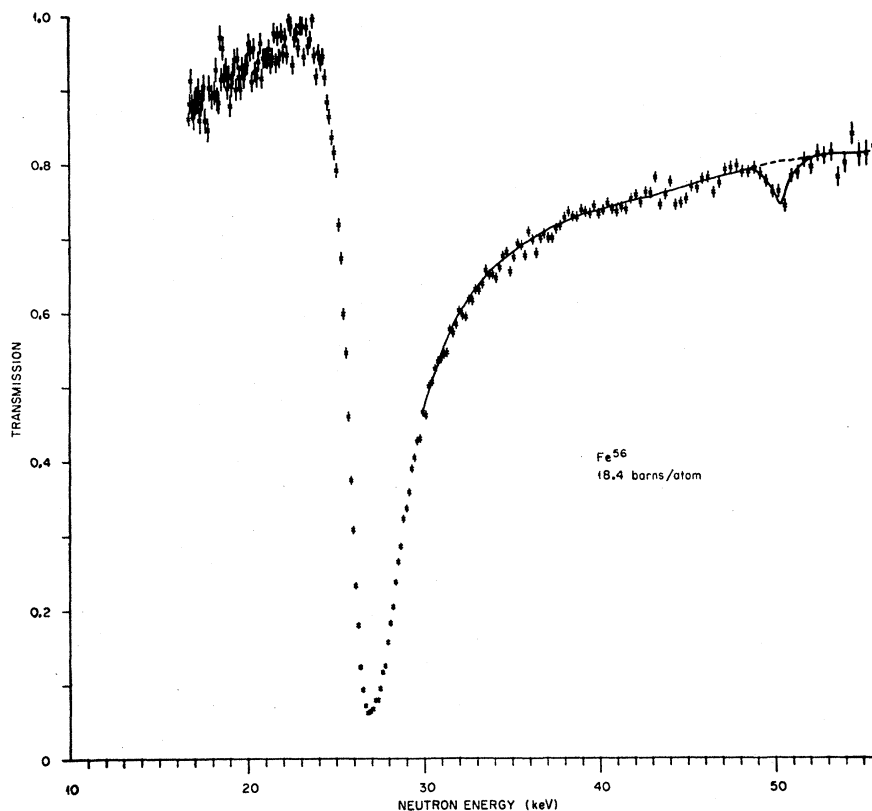
<sup>22</sup> A. G. W. Cameron, N. H. Lazar, and H. W. Schmitt, *Fast Neutron Physics* (Interscience Publishers, Inc., New York, 1963), Part II, p. 1699.

<sup>23</sup> R. L. Macklin, unpublished computer code which corrects for both scattering and resonance self-shielding effects, 1964 [see (15)].

<sup>24</sup> L. V. Groshev, A. M. Deimidov, G. A. Kotel'nikov, and V. N. Lutsenko, report from the I. V. Kurchatov Atomic Energy Institute, Moscow 1963 (unpublished).

<sup>25</sup> W. M. Good and J. H. Gibbons (private communication, 1963).

FIG. 4. Transmission versus neutron energy for  $^{56}\text{Fe}$ . The capturing states near 22 and 35 are not observed but the state near 51 keV is clearly seen in addition to the well-known resonance near 28 keV.



ferred to as astrogeriatrics) and, in general, any information on the level structure of these near-magic and magic nuclei is desirable.<sup>3-6</sup> For this reason a rather careful series of measurements was performed on the capture and total cross sections of lead isotopes. The results for  $^{206}\text{Pb}$  and  $^{207}\text{Pb}$  are included in this paper. Corresponding results for  $^{204}\text{Pb}$  and  $^{208}\text{Pb}$  will appear later.

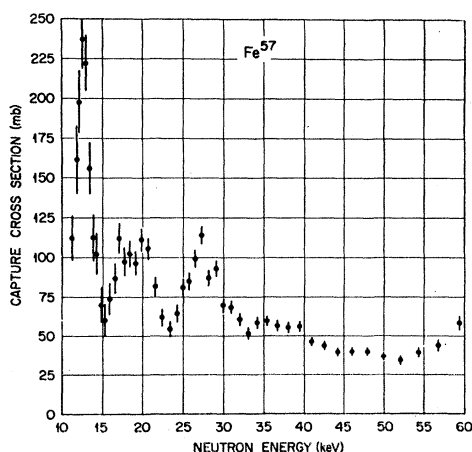


FIG. 5. Neutron capture cross section of  $^{57}\text{Fe}$ . At least three capturing resonances are seen for  $10 < E_n < 20$  keV, apparently due to resonances whose neutron scattering widths are very small.

$^{206}\text{Pb}$

Resonances in  $\sigma_T(^{206}\text{Pb}+n)$  below 200 keV have been reported<sup>8</sup> at 85, 126, 151, 188, and 197 keV. All of these resonances were assigned as due to *p*-wave neutrons. However, recent capture  $\gamma$ -ray studies<sup>9</sup> have indicated the presence of neutron-capturing states for  $(^{206}\text{Pb}+n)$  at neutron energies of about 18, 22, 27, and 45 keV.

The capture cross section for this isotope was measured using thin foils of radiogenic lead. Contribution due to  $^{207}\text{Pb}$  was subtracted by simultaneously measur-

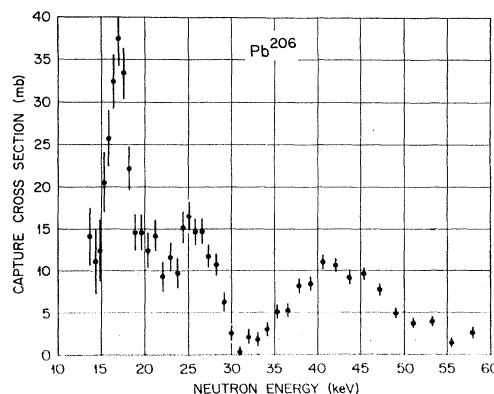


FIG. 6. Neutron capture cross section for  $^{206}\text{Pb}$ . Effects due to isotopic impurities have been removed from the results.

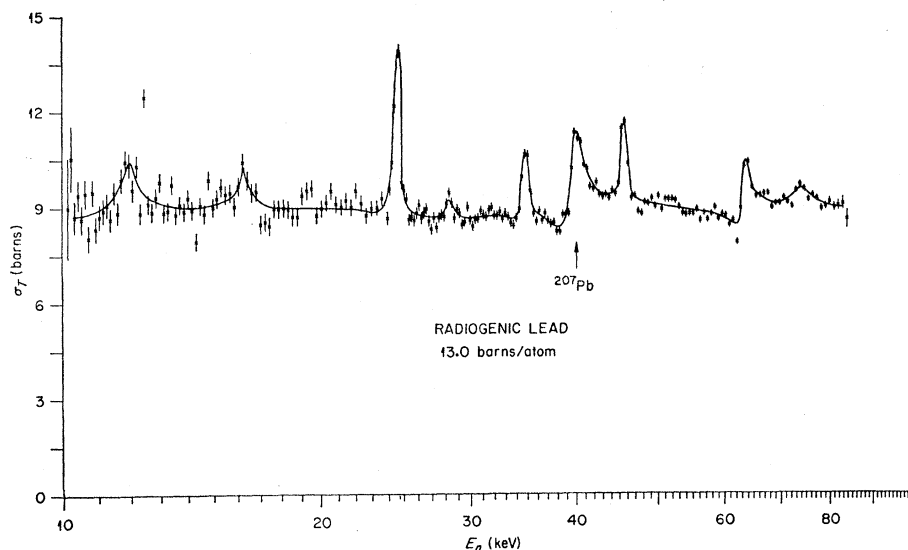


FIG. 7. Neutron total cross section for radiogenic lead (88%  $^{206}\text{Pb}$ ). The only resonance *not* due to  $^{206}\text{Pb}$  is at 42 keV, due to a strong resonance in  $(^{207}\text{Pb}+n)$ .

ing the capture cross section for samples of nearly pure  $^{207}\text{Pb}$  and  $^{208}\text{Pb}$ . The results (Fig. 6), obtained using an 8-cm flight path and consequently poor energy resolution, clearly show resonances near 17, 25, and 40 keV and possibly additional states near 20, 35, and 45 keV.

In order to understand these results better, a series of total-cross-section measurements was carried out over the same energy region with considerably better energy resolution. An average of several measurements at each energy was used to determine resonance parameters. The results from one set of runs are given in Fig. 7. The strong  $l=0$  resonance in the  $^{207}\text{Pb}$  isotopic impurity in the sample appears near 42 keV. In addition, a number of  $l \geq 1$  resonances and one  $l=0$  resonance are seen for  $^{206}\text{Pb}$ . The capture and transmission results, fully compatible with each other, are summarized in Table II. The small resonance at 75 keV is detectably distorted on its high-energy side by the 77-keV resonance in  $^{208}\text{Pb}$  (3%). The slight break in the total cross section near 20 keV was due to a poor background subtraction and is not physically significant.

If we combine these data with other available data, we can derive a value for the average level spacing. The value given by Newson *et al.*<sup>7</sup> for the average  $s$ -wave spacing is  $D_{\text{obs}}(l=0) \sim 70$  keV and more recently as  $(57 \pm 12)$  keV.<sup>26</sup> The case is not at all clear since the small  $s$ -wave strength function in this region obscures identification. We therefore conclude that  $\bar{D}_{l=0} \approx 50$  keV, since there are at least six such resonances below 350 keV. There are enough  $p$ -wave resonances for  $E_n < 80$  keV to allow an estimate of their spacing. A plot of non- $s$ -wave levels versus neutron energy is given in Fig. 8. The first resonance indicated, at  $E_n = 3.35$  keV,

was found in electron linac transmission studies.<sup>27</sup> The result,  $D_{\text{obs}}(l=1) \approx 7.5$  keV, is based on the assumption that all observed resonances except the one at 64 keV are  $p$  wave. This is a good assumption since the observed widths are reasonably clustered, the  $p$ -wave strength function is appreciable, and the centrifugal barrier for  $l=2$  versus  $l=1$  is large (a factor of about 35 for 50-keV neutrons). If we assume the spin-independent parameter  $D_0 = D_J(2J+1)$  with equal population of positive and negative parity states (i.e.  $D_{J\pi} = 2D_J$ ) we might expect to observe  $(D_{\text{obs}})_{l=1} = \frac{1}{3}(D_{\text{obs}})_{l=0}$ . However, our results (Fig. 8) indicate  $(D_{\text{obs}})_{l=1} = 7.5$  keV  $\approx (1/7)(D_{\text{obs}})_{l=0}$ . We consider this difference to be significant (outside experimental error) and conclude that the assumptions made above are not valid, at least for this nearly doubly magic nucleus. The value reported by Newson *et al.*<sup>7</sup> of  $(D_{\text{obs}})_{l=1} = 40$  keV differs from our results, probably because of their considerably lower sensitivity to such small resonances.

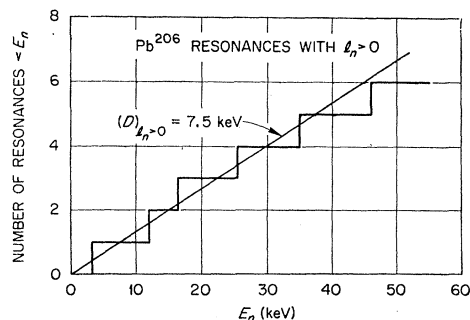
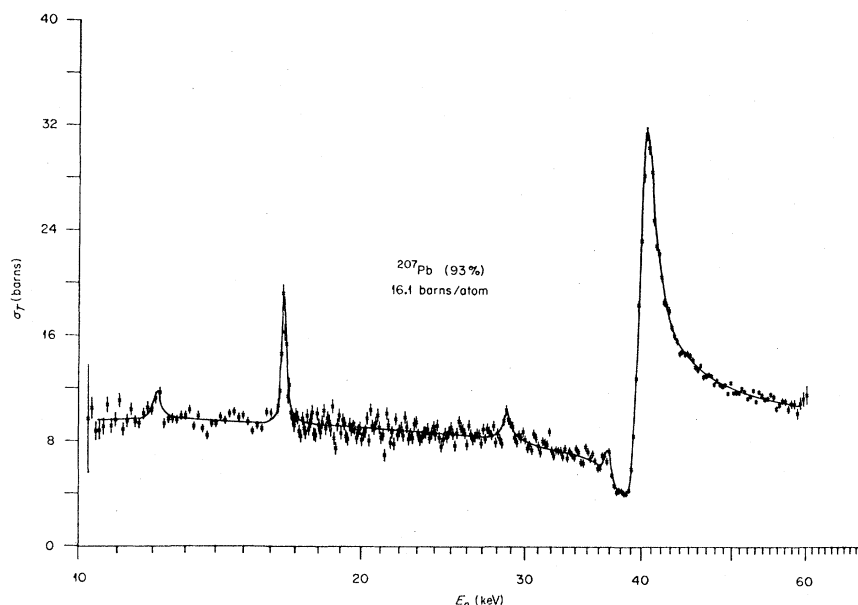


FIG. 8. Number of resonances in  $(^{206}\text{Pb}+n)$  with  $l_n \geq 1$  versus  $E_n$ . The resonances are all thought to be due to  $l_n = 1$  and result in an observed spacing of 7.5 keV, about three times smaller than expected from  $s$ -wave spacings.

<sup>26</sup> G. C. Kiker, E. G. Bilpuch, J. A. Ferrell, and H. W. Newson, *Bull. Am. Phys. Soc.* **7**, 289 (1962).

<sup>27</sup> R. C. Block and M. C. Moxon, *Bull. Am. Phys. Soc.* **8**, 513 (1963); and (private communication, 1964).

FIG. 9. Total cross section for  $(^{207}\text{Pb}+n)$ . The small resonances, due to  $l_n=1$ , were measured with two samples and at several different flight paths.



### $^{207}\text{Pb}$

Previously reported studies of resonances below 100 keV in  $(^{207}\text{Pb}+n)$  have indicated resonances at 19.6, 28.0, 44.5, 50, and 72.5 keV.<sup>7</sup> The first four resonances were assigned to  $s$ -wave neutrons and the one at 72.5 keV to  $p$ -wave neutrons. These conclusions were based on measurements with natural lead and a slightly enriched sample of  $^{207}\text{Pb}$  and are consequently quite susceptible to error. We examined both capture and total cross sections up to 60 keV and found that several of the assignments mentioned above were erroneous.

The total cross section (Fig. 9) has as its dominant feature an  $s$ -wave resonance near 41 keV. Its spin and parity ( $1^-$ ) are in agreement with earlier assignments<sup>7</sup> and have been uniquely confirmed by the observation<sup>9</sup> of capture gamma rays to the ground state ( $0^+$ ) of  $^{208}\text{Pb}$ . Such a transition would be strictly forbidden were the resonance ( $0^-$ ). Several other much weaker resonances are evident, all apparently due to  $p$ -wave neutrons. The results are summarized in Table II. The data given in Fig. 9 are illustrative of results obtained. The small resonances were measured several times under different conditions in order to obtain a value for the width.

The capture cross-section results (Fig. 10) were obtained with considerably poorer resolution, due to a much shorter neutron flight path. Resonances that dominate capture correspond to the levels near 16.5 and 43 keV. The capture peak between 30 and 35 keV is possibly due to levels at 29 and 37 but probably indicates another resonance near 33 keV as yet undetected in the total cross section. The total radiative widths for the two  $p$ -wave resonances are smaller by about a factor of 10 than the width of the single  $s$ -wave

resonance. This is not surprising since  $E1$  transition to the ground state is possible for ( $1^-$ ) capture.

A comparison of these results with those of Newson *et al.*<sup>7</sup> leads us to conclude that their assignment of levels at 19.6, 28.0, and 50.0 keV as states in  $(^{207}\text{Pb}+n)$  are, in fact, due to resonances in  $(^{207}\text{Pb}+n)$  at 16.7 and  $(^{206}\text{Pb}+n)$  at 25.1, and 46 keV. This conclusion is supported by the fact that their results using a slightly enriched  $^{207}\text{Pb}$  sample gave convincing evidence only that the 41-keV resonance was due to that isotope. We feel that the energy difference, a constant 3 keV, could be due to an early incorrect neutron-energy calibration of the Duke spectrometer.<sup>28</sup>

The over-all  $p$ -wave spacing should be equal to 4/9 of the over-all  $s$ -wave level spacing if the expression

$$D_J = \frac{D_0}{(2J+1)} = \frac{2(2I+1)}{(2J+1)} (D_{\text{obs}})_{l=0}$$

(with equal positive and negative parity populations,  $D_{J\pi} = 2D_J$ ) is valid for this nucleus. While our statistics are poor we find  $(\bar{D}_{\text{obs}})_{l=0} \approx 50$  keV and  $(D_{\text{obs}})_{l=1} \approx 8$  keV. This is three times as many  $p$ -wave levels as we might expect if the average level spacing were simply related as indicated above. This result is in good agreement with our conclusions about  $^{206}\text{Pb}$  and further strengthens the argument that for these nearly doubly magic nuclei the simple relationship between level densities of different angular momenta is not valid, or at least is dependent upon parity. These conclusions are in agreement with those of the Duke group.<sup>26</sup>

<sup>28</sup> H. W. Newson (private communication, 1958).

$^{208}\text{Pb}$ 

A very pure sample of  $^{208}\text{Pb}$  was examined for signs of resonance capture over the interval 15–60 keV. Within limits of our sensitivity ( $\pm 3$  mb) no capture occurs in this energy range. We therefore conclude that the first resonant capturing state for  $^{208}\text{Pb}$  is located above 60 keV.

*Lead Nuclear Radii*

Effective nuclear radii were obtained from the transmission curves. In the case of  $^{206}\text{Pb}$  and  $^{208}\text{Pb}$  the radius  $R'$  was obtained from values of between-resonance transmission. The values were  $(8.5 \pm 0.2)$  F and  $(8.4 \pm 0.3)$  F, respectively, where  $\sigma_{\text{pot}} \equiv 4\pi R'^2$ . This procedure was not possible in  $^{207}\text{Pb}$  because of the proximity of the large resonance at 41 keV. In that case the value of  $R'$ ,  $(9.5 \pm 0.3)$  F, was obtained from the shape fit to the resonance. These results are in relatively good agreement with an optical-model prediction of 8.7 F.<sup>29</sup>

## IV. MAXWELLIAN AVERAGED CAPTURE CROSS SECTIONS

Since capture, particularly in lead isotopes, is of special current interest in cosmology we have computed for the data presented here the average cross section corresponding to neutrons in a temperature distribution of average energy  $kT$ . The results are presented in Fig. 11.

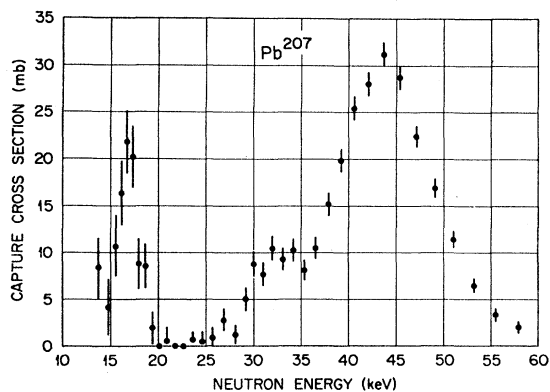


FIG. 10. Capture cross section for  $^{207}\text{Pb}$ . The capture results are consistent with the total-cross-section results, but indicate the probable presence of an additional resonance near 33 keV.

<sup>29</sup> F. Perey (private communication).

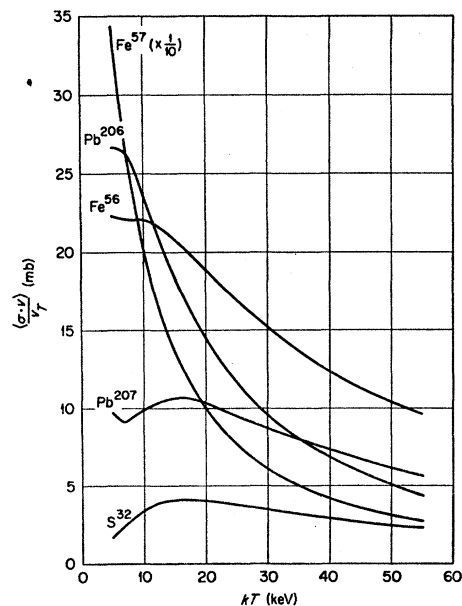


FIG. 11. Capture cross sections averaged over a Maxwellian neutron temperature distribution of average energy  $kT$ .

## V. CONCLUSIONS

The results given in this paper point out the fact that capture in the resonance region is frequently dominated by resonances that are virtually unobservable in transmission. The presence of several very narrow resonances in studies of iron may be evidence of  $d$ -wave interactions below 50 keV. The studies of  $^{206}\text{Pb}$  and  $^{207}\text{Pb}$  strongly suggest that in these near-magic nuclei the often assumed relation  $D_J = D_0 / (2J + 1)$  is not adequate. A large differential (a factor of 10) in radiative width for  $p$ -wave versus  $s$ -wave (of the type  $1^-$ ) capture in  $^{207}\text{Pb}$ , is apparently due to the strong  $E1$  ground-state transition.

## ACKNOWLEDGMENTS

We are grateful for the active collaboration of many of our colleagues at ORNL during the course of these measurements. The contributions of J. A. Biggerstaff, W. M. Good, J. P. Judish, and M. Nushan were particularly valuable. Discussions with R. C. Block and H. W. Newson were very helpful. One of us (P.J.P.) is indebted to the Netherlands *Stichting voor Fundamenteel Onderzoek der Materie (F.O.M.)* for financial support. He would also like to acknowledge the kind hospitality of ORNL during his temporary stay.